



ELSEVIER

Biophysical Chemistry 103 (2003) 201–211

Biophysical
Chemistry

www.elsevier.com/locate/bpc

Kinetic analysis of artificial peptide self-replication. Part II: The heterochiral case

Jesús Rivera Islas^a, Véronique Pimienta^b, Jean-Claude Micheau^b, Thomas Buhse^{a,*}

^aCentro de Investigaciones Químicas, Universidad Autónoma del Estado de Morelos, Av. Universidad N° 1001, Col. Chamilpa, 62210 Cuernavaca, Morelos, Mexico

^bLaboratoire des IMRCP, UMR au CNRS N° 5623, Université Paul Sabatier, 118, route de Narbonne, F-31062 Toulouse Cedex, France

Received 28 June 2002; received in revised form 7 August 2002; accepted 15 August 2002

Abstract

A kinetic model has been designed to describe and to analyze the stereoselective behavior of a recently discovered heterochiral template-directed peptide self-replicator by Ghadiri and co-workers [Nature 409 (2001) 797–801]. It turned out that previous assumptions stating that exclusively homochiral species participate in a stereoselective and autocatalytic pathway and that heterochiral species originate only from uncatalyzed background reactions could not be validated by our model. On the contrary, excellent fitting of experimental data indicated that the whole combinatorial variety of possible cross-catalytic processes involving L- and D- peptide species play an important role and need to be taken into account. The system shows no net creation of chiral matter but only a redistribution of the initially present chiral material. Both, the separation of an optically inactive *meso*-type template dimer and a slight chiroselective autocatalytic effect, contribute to a predicted amplification of enantiomeric excess that, in some cases, can simultaneously result in a substantial amount of optically active matter.

© 2002 Elsevier Science B.V. All rights reserved.

Keywords: Self-replication; Peptide; Kinetic analysis; Autocatalysis; Stereoselectivity; Amplification of enantiomeric excess; Biomolecular homochirality; Chiroselective autocatalytic effect

1. Introduction

Molecular self-replication, joined by a high degree of stereospecificity, is the essential attribute of living systems. In the search for the origins of life, artificial self-replicating systems have played a key role to obtain a closer insight into prebiotic scenarios from which complex biomolecules and

their actions have presumably emerged [1–4]. An understanding of chiral implications in these systems can give further possible clues into the direction of the origin of biomolecular homochirality [5–8], which is still — together with the origin of life — one of the most challenging open questions to the scientific community.

Self-replicating systems show per definition [9] non-linear kinetics, although typically with a drastically reduced autocatalytic efficiency [10]. In the recent years, specific autocatalytic reaction systems

*Corresponding author. Tel.: +52-777-3-29-79-97; fax: +52-777-3-29-79-97.

E-mail address: buhse@uaem.mx (T. Buhse).

that involve chiral molecular or supramolecular entities have been reported to exhibit spontaneous amplification of enantiomeric excess up to complete breaking of the chiral symmetry [11–14]. These processes normally occur when the chiral product species acts as a catalyst of its own formation, which is commonly referred to as stereospecific autocatalysis. However, it has been shown that autocatalysis alone can not produce this effect but additionally needs a considerably high degree of stereoselectivity [15] as well as the involvement of so-called mutual inhibition [16,17] for the case of entire chiral symmetry breaking phenomena. This is certainly the reason why this type of reaction systems is extremely rare. The effect of stereospecific autocatalysis has been almost exclusively observed in cases in which nucleation or aggregation effects take place [14,18] or in which autocatalytic species with highly stereospecific ligation capacities are involved [14,19,20]. In this sense, self-replicating systems — that a priori exhibit both autocatalytic kinetics as well as a high potential for chiral recognition — can be regarded as promising candidates to generate chiral amplification. Furthermore, in the case of prebiotically relevant self-replicating systems, a positive outcome could directly be related to a possible prebiotic scenario at a time in which molecular evolution turned from an almost racemic into the current homochiral state of Earth's biosphere.

In a previous paper [21], we presented a theoretical kinetic analysis of a peptide-based self-replicator that has been discovered by Ghadiri and co-workers [22,23]. Our kinetic analysis and modeling addressed to a reaction system, in which two short peptide fragments (E and N) of almost the same chain length combine by peptide bond linkage to form a product (T) that was shown to catalyze in a template-directed fashion the linkage between E and N and by that its own formation in an autocatalytic way. Ghadiri's experiments as well as our subsequent kinetic modeling referred in this case to an entirely homochiral scenario involving exclusively naturally based L-amino acid building blocks. We introduced a 6-step kinetic model for this system that gave rise to excellent fitting of 4 independent experimental series and

that illustrated a number of basic dynamic principles of this self-replicator.

As an extension of this work, we will present in this publication a kinetic analysis of this self-replicator that is additionally exposed to heterochiral conditions, i.e. in which L- as well as D-reactant species were present. Our analysis is based on a recent experimental study by Ghadiri and co-workers in which an astonishing effect of stereoselectivity has been reported [24]. These studies were performed under very similar conditions as already described for the homochiral case [22,23] but with the further impact of using four instead of two different reactant species: an electrophilic peptide fragment composed of L-amino acids (EL) and the respective composite with exactly the same sequence made of D-amino acids (ED) as well as the two enantiomeric nucleophilic and homosequential counterparts (NL and ND). Possible monomeric product species under these conditions were two homochiral template products (TLL and TDD) and two heterochiral ones (TLD and TDL).

Ghadiri and co-workers found that the formation of the homochiral template species TLL and TDD was kinetically favored over the formation of the heterochiral species TLD and TDL, which leads to a pronounced bias in the product distribution at the end of the experimental time in the form of $[(TLL + TDD)] > [(TLD + TDL)]$. This clearly indicated a chiroselective effect in this system that was probably assisted by the underlying autocatalytic kinetics. A first explanation, which was supported by a number of sub-system experiments [24], indicated that only the homochiral template species participated in the autocatalytic cycle such as assumed for the former homochiral system but that the heterochiral template species were exclusively generated by uncatalyzed background reactions.

The above experimental outcome has been discussed in terms of a possible explanation for the origin of biomolecular homochirality [24]. We will analyze the dynamic properties of this reaction system in a similar approach like in the previous paper [21] and also try to predict its possible capacity to generate a bias concerning the concentrations of enantiomeric species by a chiroselective autocatalytic effect.

Table 1

Experiments taken under consideration for the modeling approach. $[E]_0 = [N]_0 = 100 \mu\text{M}$, $[\text{TLL}]_0 = 25 \mu\text{M}$ (exp. 4), $[\text{BnSH}]$ (benzyl mercaptan) $\cong 91 \text{ mM}$, $[\text{MOPS}]$ [3-(*N*-morpholino)-propanesulfonic acid] = 100 mM. $T = 21 \text{ }^\circ\text{C}$ (from ref [24]).

| Experiment number | Reactants | Product templates |
|-------------------|----------------|--------------------|
| 1 | EL, NL, ED, ND | TLL, TLD, TDL, TDD |
| 2 | ED, NL | TDL |
| 3 | EL, NL | TLL |
| 4 | EL, NL, TLL | TLL |

Table 2

List of species involved in the kinetic model of the heterochiral Ghadiri system. The table displays their content of L-matter (%). The 50% column acts as the mirror indicating the enantiomeric pairs on the right and on the left of it. 0% of L-matter corresponds to 100% of D-matter

| L-matter (%) | 100 | 75 | 66.6 | 50 | 33.3 | 25 | 0 |
|-------------------------------|---------|--------------------|----------------------------|--|----------------------------|--------------------|---------|
| Electrophilic fragment | EL | | | | | | ED |
| Nucleophilic fragment | NL | | | | | | ND |
| Homochiral template monomer | TLL | | | | | | TDD |
| Heterochiral template monomer | | | | TLD TDL | | | |
| Templated E | TLL–EL | | TLL–ED TLD–EL TDL–EL | | TDD–EL TDL–ED TLD–ED | | TDD–ED |
| Templated N | TLL–NL | | TLL–ND TLD–NL TDL–NL | | TDD–NL TDL–ND TLD–ND | | TDD–ND |
| Template dimer | TLL–TLL | TLL–TLD TLL–TDL | | TLD–TLD TLD–TDL TDL–TDL TLL–TDD | | TDD–TDL TDD–TLD | TDD–TDD |

2. Kinetic modeling

2.1. Selection of experimental data

We considered for our approach 4 experiments from the published experimental data [24] in which in all cases peptide fragments of identical amino acid sequence and equal experimental conditions have been applied. This allowed us to compare directly these different experiments and to attempt a multi-experiment data fitting, i.e. the search for a unique set of rate parameters for all experimental

scenarios. The 4 experiments are summarized in Table 1.

Experiment (1) starts with equimolar amounts of the 4 reactant species where the time evolution of the combined product concentrations, homo = $[(\text{TLL}) + (\text{TDD})]$ and hetero = $[(\text{TLD}) + (\text{TDL})]$, has been experimentally monitored. It resulted at the end of the experimental reaction time in a diastereomeric excess in favor of the homo species of close to 70%, $de = \{[(\text{TLL}) + (\text{TDD})] - [(\text{TLD}) + (\text{TDL})]\} / [\text{T}]_{\text{total}} \cong 0.7$. The analytical technique used by Ghadiri and co-workers only

allowed to distinguish between diastereomers but not between enantiomers. Hence there was no experimental information available about the time evolution of a single enantiomeric species. Experiment (2) starts with equimolar amounts of ED and NL but without EL and ND so that the only possible product species is TDL. Experiments (3) and (4) were homochiral reference experiments with TLL as the exclusive product species such as described previously [21].

The selected experiments cover the possible cases of chiral cross interactions (1), purely heterochiral (2) or homochiral interactions (3) as well as the expected catalytic effect of an initially present homochiral template species (4).

2.2. Chiral combinatorics: the kinetic model

Preliminary attempts to reproduce the data of experiments (1–4) simultaneously were done with basically the former 6-step kinetic scheme [21] that has been adapted to the heterochiral case. We followed the possible explanation that TLL and TDD were generated via an autocatalytic pathway but TLD and TDL only by uncatalyzed background reactions and that no homo/hetero cross-catalytic processes occurred. These attempts did not result in an acceptable data fitting indicating a higher complexity of the reaction network. For that reason, a combinatorial approach was chosen that includes a larger number of possible elementary steps and does not exclude a priori any cross-catalytic effects.

Table 2 shows the involved species taken into account for our kinetic model. Considering a dimerization of the template species, the number of species grows significantly from formerly 6 to 34 in the heterochiral case. For instance, the formation of the intermediates TE and TN give rise to 16 different species by the combinatorial approach while there were only 2 different one considered for the homochiral model [21].

Due to the chiral combinatorics, also a considerable increase in the number of steps from 6 for the homochiral case to 62 for the heterochiral case arises. As a basic assumption for the chiral combinatorics, we allowed stereoselectivity (i.e. chiral

recognition) for all second-order reactions while first-order processes have been considered not to be stereoselective. Homochiral interactions like L+L or D+D are called *even* and the heterochiral ones of the type D+L are indicated by *odd*. This concept is translated for the values of the rate constants allowing disparity for the second-order rate constants:

$$k_{(\text{second-order})\text{even}} \neq k_{(\text{second-order})\text{odd}}.$$

The same type of reactions exclusively considering mono- or bimolecular processes as in ref. [21] has been considered:

- I. $E + N \rightarrow T$ (irreversible formation of the template).
- II. $T + X \rightleftharpoons TX$ (reversible template-fragment association equilibrium, $X = E$ or N).
- III. $TX + Y \rightarrow TT$ (irreversible catalyzed formation of the template dimer, $X = E$ if $Y = N$ or $X = N$ if $Y = E$).
- IV. $T + T \rightleftharpoons TT$ (reversible template–template association equilibrium).

Table 3 indicates the processes, rate constants and how the *even* and *odd* notation has been applied in particular.

Fig. 1 represents the basic complex structure of the chiral combinatorics in a schematized manner. The complete kinetic scheme including all elementary processes and the corresponding rate constants is provided as supplementary material.

2.3. Computational procedures

Model calculations were performed with Sa (version 2.0) [25] on a Pentium III personal computer based on a semi-implicit Runge–Kutta method. The basic procedure of fitting experimental data using a non-linear minimization algorithm for the fitting between the model and the data has been already described previously [21]. Fitted rate parameters were automatically and iteratively returned to the numerical integration until a minimum in the residual error was reached. The robustness of the solution was evaluated by showing that, whatever the guessed initial values were,

Table 3

Rate constants, processes and optimized values of the rate parameters obtained by simultaneous fitting of experiments (1) to (4) of the heterochiral Ghadiri system. Note that the chiral combinatorics conditions apply only on the bimolecular processes. ($i, j, k, m = D$ or L ; if $X = E$ then $Y = N$ and conversely). Rate laws are written in the usual way. k_1 and k_3 correspond to the irreversible covalent template formation. k_2 and k_4 are involved in template-building block or template-template reversible association whose respective reverse processes are characterized by k_{-2} and k_{-4} .

| Second-order rate constants ($M^{-1} s^{-1}$) | Type of reaction | Chiral combinatorics conditions | Number of processes | Optimized values of the rate parameters ($M^{-1} s^{-1}$) |
|---|--|---|---------------------|---|
| $k_{1\text{even}}$ | $E_i + N_j \rightarrow T_{ij}$ | $\forall i, j \ i=j$ | 2 | 0.14 |
| $k_{1\text{odd}}$ | $E_l + N_j \rightarrow T_{ij}$ | $\forall i, \ j \ i \neq j$ | 2 | 2.6×10^{-2} |
| $k_{2\text{even}}$ | $T_{ij} + X_k \rightarrow T_{ij}X_k$ | $X = E$ and $i = k$ or $X = N$ and $j = k$ | 8 | 25.8 |
| $k_{2\text{odd}}$ | $T_{ij} + X_k \rightarrow T_{ij}X_k$ | $X = E$ and $i \neq k$ or $X = N$ and $j \neq k$ | 8 | 8.7×10^{-2} |
| $k_{3\text{even}}$ | $T_{ij}X_k + Y_m \rightarrow T_{ij}T_{km}$ | $X = E$ and $j = m$ or $X = N$ and $i = m$ | 16 | 1.2×10^4 |
| $k_{3\text{odd}}$ | $T_{ij}X_k + Y_m \rightarrow T_{ij}T_{km}$ | $X = E$ and $j \neq m$ or $X = N$ and $j \neq m$ | 16 | 2.2×10^3 |
| $k_{4\text{even-even}}$ | $T_{ij} + T_{km} \rightarrow T_{ij}T_{km}$ | $i = k$ and $j = m$ | 4 | 5.7×10^4 |
| $k_{4\text{even-odd}}$ | $T_{ij} + T_{km} \rightarrow T_{ij}T_{km}$ | $i = k$ and $j \neq m$ or $i \neq k$ and $j = m$ | 4 | 5.7×10^7 |
| $k_{4\text{odd-odd}}$ | $T_{ij} + T_{km} \rightarrow T_{ij}T_{km}$ | $i \neq k$ and $j \neq m$ | 2 | 3.2×10^5 |
| First-order rate constants (s^{-1}) | | | | (s^{-1}) |
| k_{-2} | $T_{ij}X_k \rightarrow T_{ij} + X_k$ | none | $8 + 8 = 16$ | 0.24 |
| k_{-4} | $T_{ij}T_{km} \rightarrow T_{ij} + T_{km}$ | none | $4 + 4 + 2 = 10$ | 7.1×10^{-4} |

same parameter values were delivered at convergence.

2.4. Numerical data fitting

Fig. 2 shows the multi-experiment fitting of the selected experiments. The result indicates a satisfactory correspondence between the model and the two heterochiral and two homochiral experimental scenarios. It supports the basic mechanistic principle of template-directed self-replication as already discussed [21] but also indicates that cross-catalytic chiral interactions for the heterochiral case are not negligible.

The data fitting was based on the assumption that at the time the reaction was experimentally quenched and the product concentrations were chromatographically determined, all non-covalent associations underwent complete dissociation. Thus the product concentrations as shown by Ghadiri and co-workers [24] were considered to

be the sum of all homochiral vs. heterochiral T species.

2.5. Semi-quantitative estimation of the rate parameters

Table 3 shows the obtained rate parameters for the heterochiral setting by simultaneous fitting of four experiments. The values demonstrate acceptable coherence within the order of magnitude to the values of the rate parameters found for the homochiral case [21] in which only *even* type processes were considered. This indicates that the same basic mechanism applies for both experimental scenarios, i.e. homochiral experiments can be understood as a special case of the more general heterochiral case.

Concerning the stereoselectivity of the processes, we found that the covalent ligation, $E + N \rightarrow T$, is stereoselective in the sense that the homochiral (*even*) ligation ($EL + NL$) is approxi-

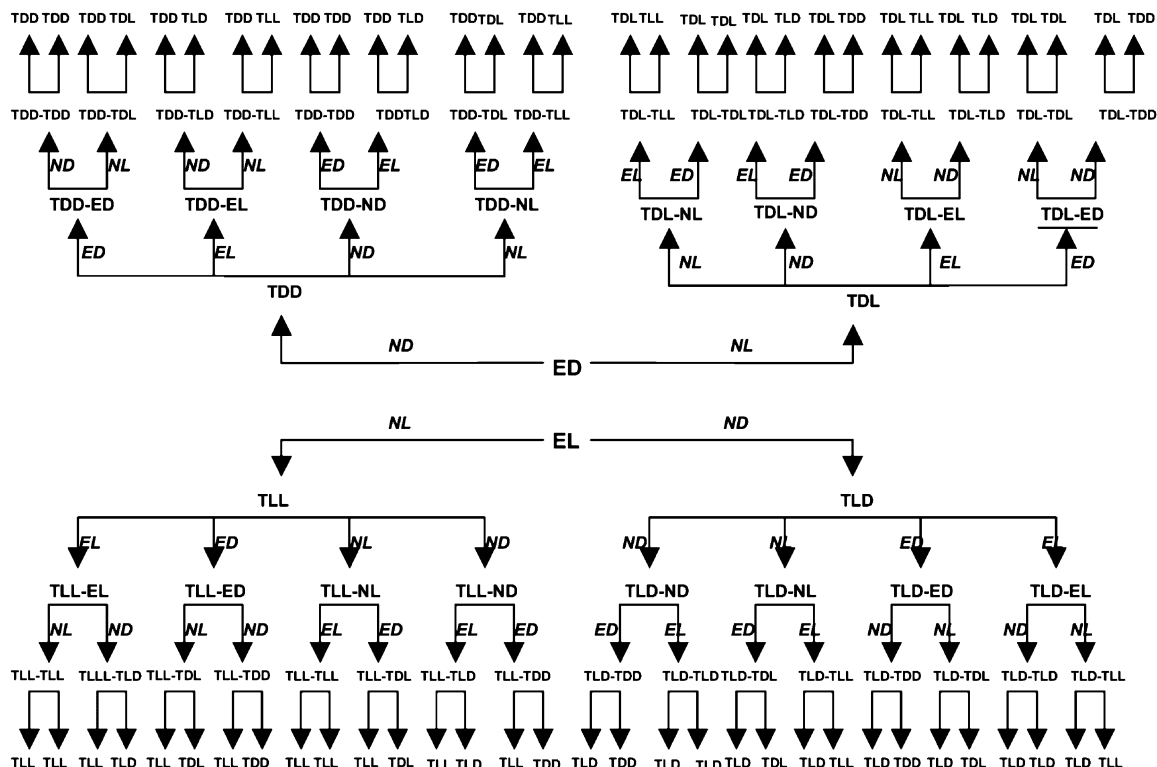


Fig. 1. Schematic outline of the kinetic model after applying chiral combinatorics. For the sake of clarity, reversible processes have not been indicated.

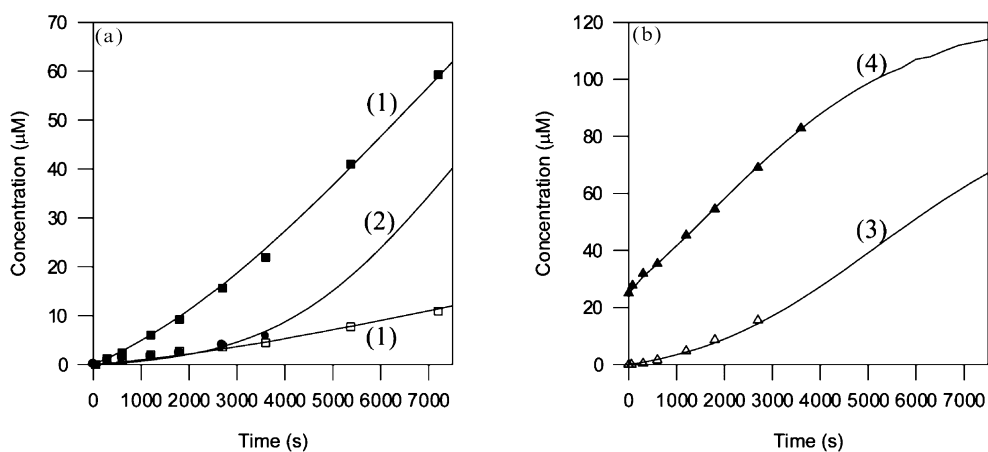


Fig. 2. Product formation vs. time of experiments (1–4) of chiroselective peptide self-replication. The continuous lines show the numerical fitting of the published [24] experimental data (marks). Graph (a) represents the heterochiral experiments (1) $\text{EL} + \text{NL} + \text{ED} + \text{ND} \rightarrow (\text{TLL} + \text{TDD})$ (■) + $(\text{TLD} + \text{TDL})$ (□) and (2) $\text{ED} + \text{NL} \rightarrow \text{TDL}$ (●). Graph (b) shows the homochiral control experiments (3) $\text{EL} + \text{NL} \rightarrow \text{TLL}$ (Δ) and (4) $\text{EL} + \text{NL} + \text{TLL} \rightarrow \text{TLL}$ (\blacktriangle), $[\text{TLL}]_0 = 25 \mu\text{M}$. Initial concentrations for all peptide fragments = 100 μM .

mately 5 times faster than the heterochiral (*odd*) ligation. In this respect, the formation of the homochiral species is kinetically favored already in the uncatalyzed direct formation of the template. The same trend — considerably more pronounced — is also observed for the hydrophobic side association, $T + X \rightarrow TX$, in which the *even* processes occur approximately 300 times faster than the *odd* associations. The hydrophobic side association and catalyzed ligation, $TX + Y \rightarrow TT$, is also stereoselective, however, to a lesser extent: the *even* processes are approximately 6 times faster. These results so far show that the hypothesis made by Ghadiri and co-workers [24] that the homochiral processes are kinetically favored over the heterochiral ones is in agreement with our fitting results. We also showed that these interactions are not stereospecific, but only stereoselective.

Concerning the hydrophobic dimerization, $T + T \rightarrow TT$, a more complex situation was observed. From our results, it turns that *even-odd* dimerizations are drastically favored (approx. 1000 times) over the *even-even* dimerizations and that they are also favored (approx. 200 times faster) over the *odd-odd* dimerizations.

Tentatively, we interpret these effects to be governed by differences in the structural geometries between the different template molecules that affect the strength of the intermolecular hydrophobic attraction [26,27] and finally the rate of these processes. Due to the absence of particular experimental data, structural arguments have not been included in the model and are beyond the scope of the present work.

3. Dynamic features of the heterochiral Ghadiri system

3.1. The chiroselective effect and amplification of enantiomeric excess

When started under racemic conditions, $[EL]_0 = [ED]_0 = [NL]_0 = [NL]_0$, experimental studies clearly demonstrated an increase of the diastereomeric excess during the course of the reaction [24]. In respect to the model, this effect is reflected by our fitting that shows the diverging time evolution of homochiral vs. heterochiral product species. But

under these conditions and under the assumption that the system is chirally insensitive to fluctuations (i.e. in which a small random enantiomeric excess is not greatly amplified [14]), no bias in the concentrations of the enantiomeric pairs can evolve. Thus according to the initial conditions, the enantiomeric excess (*ee*),

$$ee(\%) = \frac{([L] - [D])}{([L] + [D])} \times 100$$

for all species will remain at zero, where L and D denote the respective enantiomeric pairs as indicated in Table 1.

In the presence of non-racemic initial conditions, differences in the time evolution of enantiomeric species can be expected. However, in the Ghadiri system, no net creation of chiral material takes place but initially present chiral matter is redistributed over the number of product species. This is fundamentally different to prototype systems of stereospecific autocatalysis [11–14] in which the concentration of chiral matter increases during the reaction because it was generated from an achiral substrate. Hence, for the Ghadiri system, the examination of the enantiomeric excess alone can be misleading since it may be associated to enantiomeric annihilation like in a racemate crystallization [28–30] resulting in an high enantiomeric excess but also in extremely small quantities of chiral matter. For that reason, the optical yield as the concentration difference between L- and D-matter in respect to the enantiomeric pairs (see Table 2) should also be taken into account.

As shown in Table 4, model simulations in respect to the equilibrium distribution of the enantiomeric species can result in a net amplification of the initial enantiomeric excess.

Maximum final values for the enantiomeric excess (positive or negative) frequently correspond to extremely low values in the optical yield. But also chiral amplification effects from $ee_0 = \pm 5\%$ to $ee_{eq} = \pm 19.0-28.6\%$ are observed that go along with a significant amount of optically active matter.

After our numerical simulations, we could find in general that the product distribution follows the order $[TT] \gg [T] > [TX]$. The main end product

Table 4

Model predictions for final values of the enantiomeric excess (%) after simulations under selected non-racemic initial conditions in which (a) one building block is racemic and the other non-racemic, (b) both building blocks have the same initial enantiomeric excess, and (c) the building blocks have an opposite enantiomeric excess. Values in brackets refer to the corresponding optical rotation, $[L]-[D]$ (μM), in respect to the final concentrations of the enantiomeric pairs such as indicated in Table 2 [e.g. (TLL–TLD)-(TDD–TDL)]. Note the cases in which simultaneously enantiomeric excess amplification and a substantial amount of optically active matter are obtained (most significant values are in bold).

| Concentrations (μM) | (a) | (b) | (c) |
|----------------------------------|----------------------------------|---------------------------------|-----------------------------------|
| $[\text{EL}]_0$ | 105 | 105 | 105 |
| $[\text{ED}]_0$ | 95 | 95 | 95 |
| $[\text{NL}]_0$ | 100 | 105 | 95 |
| $[\text{ND}]_0$ | 100 | 95 | 105 |
| Enantiomeric excess (%) | | | |
| E (initial) | 5 | 5 | 5 |
| N (initial) | 0 | 5 | –5 |
| TLL (eq) | 4.8 (3.2×10^{-2}) | 9.6 (6.4×10^{-2}) | 0 (0) |
| TLD (eq) | 15.0 (9.5×10^{-5}) | 0 (0) | 28.6 (1.92×10^{-4}) |
| TLL–TLL (eq) | 9.6 (1.68) | 19.0 (3.39) | 0 (0) |
| TLL–TLD (eq) | 19.6 (3.30) | 9.6 (1.58) | 28.6 (5.0) |
| TLL–TDL (eq) | –10.2 (–1.69) | 9.6 (1.58) | –28.6 (–5.0) |
| TLD–TLD (eq) | 29.3 (4.8×10^{-6}) | 0 (0) | 52.9 (1.02×10^{-5}) |

appears to be the racemic (*meso*-type) template dimer TLL–TDD. The formation of this species, which is gathering chiral matter to an optically inactive product and increasing the enantiomeric excess of the remaining chiral species, stands for the main reason for the observed amplification of enantiomeric excess. The racemate separation type process is illustrated in Fig. 3 for arbitrarily chosen non-racemic initial conditions.

However, as discussed in the following section by focusing on the dynamics of the product evolution, racemate separation can not be the single cause for the predicted amplification of enantiomeric excess.

3.2. Time evolution of the main species and the chiroselective autocatalytic effect

Fig. 4 shows the simulated time evolution of the reactant species E and N. Initially the concentration of L-matter is higher than D-matter. However, D-matter becomes in excess after

approximately 30% of reaction extent. This is clearly the manifestation of a chiroselective autocatalytic effect in which the consumption of L-matter is autocatalytically accelerated by L-matter and consequently the D-matter of the building blocks reacts retarded. Further approaching 100% extent of reaction, D-matter finishes to be consumed and the difference decreases but depending on the initial conditions some building block matter remains unreacted.

As indicated in Fig. 5, the initially present relative enantiomeric mass difference between L- and D- matter remains constant but will be redistributed over all species during the reaction.

The total L-matter as shown in Fig. 5, which is located at the beginning of the experiment in the building blocks EL and NL, will be redistributed mainly over the template dimer species as the reaction proceeds. The specific distribution pattern depends on the initial conditions. In the given example and between 40 and 75% of reaction extent, the major L-matter containing species is

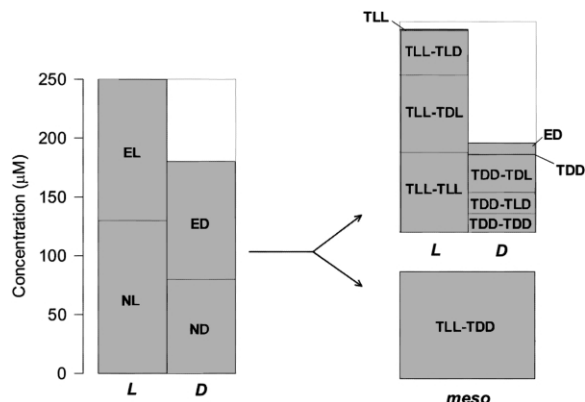


Fig. 3. Simulation demonstrating redistribution of chiral matter and amplification of enantiomeric excess in the heterochiral Ghadiri system. Columns on the left illustrate the arbitrarily chosen initial conditions $[EL]_0 = 120 \mu\text{M}$, $[NL]_0 = 130 \mu\text{M}$, $[ED]_0 = 100 \mu\text{M}$, and $[ND]_0 = 80 \mu\text{M}$ giving rise to $ee_0 = 16.3\%$ in respect to L-matter. The columns on the upper right (same scale) show the final distribution of the optical active products resulting in an apparent amplification of enantiomeric excess to $ee_{eq} = 39.1\%$. The column on the lower right shows the concentration of the optically inactive *meso* product TLL–TDD. Note that the product distribution follows in this case the order $[TT_{meso}] > [\text{other TT's}] > [ED] > [T's] > [\text{all TX}]$.

the homochiral TLL–TLL. In the later stages of the reaction, however, the *meso*-type dimer TLL–TDD becomes together with other dimers one of the dominating compounds.

4. Conclusion

We presented the first kinetic analysis of a stereoselective peptide self-replicator. The fitting of experimental data by our combinatorial modeling approach indicates that the former homochiral Ghadiri system can be regarded as a special case of the presently examined heterochiral case. In this respect, our previous conclusions about the basic dynamics of this self-replicator hold for both cases.

Stereoselective actions apparently occur in each of the bimolecular steps that were taken under consideration. This indicates that chiral cross-interactions between homo- and heterochiral species have to be taken into account.

The reaction system is operating with an initially present chiral pool but does not generate additional

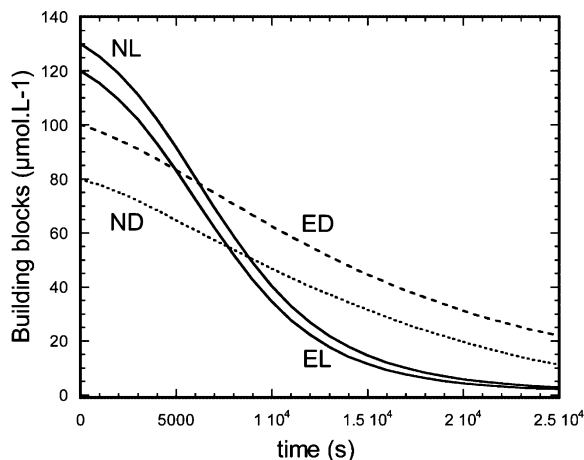


Fig. 4. Simulation showing the time evolution of the building block species. Note the rapid consumption of the building blocks that were initially the higher concentrated ones. This effect is the signature of an autocatalytic process. Initial conditions are like in Fig. 3.

chiral matter. Because of this, amplification of enantiomeric excess with simultaneous generation of a considerable yield of optically active material, is fundamentally limited.

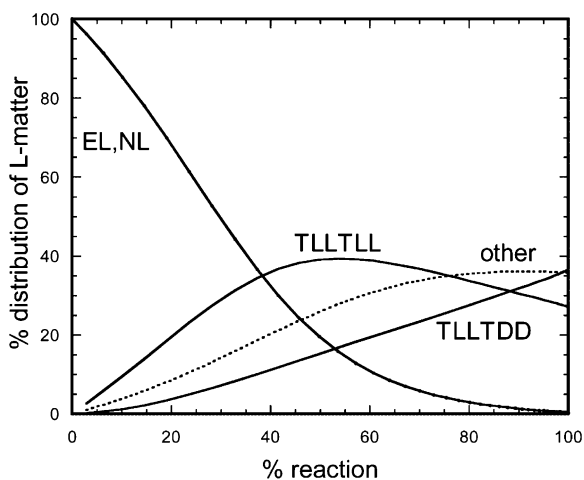


Fig. 5. Simulation showing the redistribution of initial L-matter as a function of the reaction extent (%). ‘Other’ indicates all other heterodimers like TLL–TLD, TLD–TLD, TDD–TDL, etc. Initial conditions are like in Fig. 3.

Chiral amplification effects that have been observed by our simulations are mainly due to the formation of *meso*-like species. This indicates characteristic similarities between the chiral processing of this system and processes of racemate crystallization. Both have in common to produce typically high enantiomeric excess that is accompanied by an almost total loss of optically active matter.

However, our simulations also predict the presence of a chiroselective autocatalytic effect that—in some cases—generates indeed an enantiomeric excess and still a significant amount of optically active matter at the same time. The relative importance between chiral autocatalysis and *meso*-separation obviously depends on the initial conditions.

Further laboratory experiments screening the enantiomeric excess and the amount of optically active matter under non-racemic initial conditions could give closer insight into the chiral combinatorics and finally answer the question for chiral amplification effects in a more definite way.

5. Supplementary material

Supplementary material is available from the author upon request.

Acknowledgments

This work was funded by a bilateral Mexican-French cooperation project (CONACyT-CNRS grant E130.1135/2001). T.B. and J.R.I. also acknowledge gratefully financial support from the CONACyT research project program (grant 34236-E).

References

- [1] S.F. Mason, *Chemical evolution*, Clarendon Press, Oxford, 1991.
- [2] L.E. Orgel, *Molecular replication*, *Nature* 358 (1992) 203–209.
- [3] B.G. Bag, G. von Kiedrowski, *Templates, autocatalysis and molecular replication*, *Pure Appl. Chem.* 68 (1996) 2145–2152.
- [4] A. Robertson, A.J. Sinclair, D. Philp, *Minimal self-replicating systems*, *Chem. Soc. Rev.* 29 (2000) 141–152.
- [5] W.A. Bonner, *The origin and amplification of biomolecular chirality*, *Origins Life Evol. Biosphere* 21 (1991) 59–111.
- [6] L. Keszthely, *Origin of the homochirality of biomolecules*, *Q. Rev. Biophys.* 28 (1995) 473–507.
- [7] G. Pályi, C. Zucchi, L. Caglioti (Eds.), *Advances in biochirality*, Elsevier, Amsterdam, 1999.
- [8] M. Avalos, R. Babiano, P. Cintas, J.L. Jiménez, J.C. Palacios, *From parity to chirality: chemical implications revisited*, *Tetrahedron Asymmetry* 11 (2000) 2845–2874.
- [9] D.N. Reinhoudt, D.M. Rudkevich, F. de Jong, *Kinetic analysis of the Rebek self-replicating system: is there a controversy?*, *J. Am. Chem. Soc.* 118 (1996) 6880–6889.
- [10] G. von Kiedrowski, *Minimal replicator theory I: parabolic vs. exponential growth*, *Bioorg. Chem. Front.* 3 (1993) 113–146.
- [11] M. de Min, G. Levy, J.C. Micheau, *Chiral resolutions, asymmetric synthesis and amplification of enantiomeric excess*, *J. Chim. Phys.* 85 (1988) 603–619.
- [12] M. Avalos, R. Babiano, P. Cintas, J.L. Jiménez, J.C. Palacios, *Non-linear stereochemical effects in asymmetric reactions*, *Tetrahedron Asymmetry* 8 (1997) 2997–3017.
- [13] C. Girard, H.B. Kagan, *Non-linear effects in asymmetric synthesis and stereoselective reactions: ten years of investigation*, *Angew. Chem. Int. Ed. Engl.* 37 (1998) 2922–2959.
- [14] D.K. Kondepudi, K. Asakura, *Chiral autocatalysis, spontaneous symmetry breaking, and stochastic behavior*, *Acc. Chem. Res.* 34 (2001) 946–954.
- [15] T. Buhse, D. Lavabre, J.C. Micheau, W. Thiemann, *Chiral symmetry breaking: experimental results and computer analysis of a liquid-phase autoxidation*, *Chirality* 5 (1993) 341–345.
- [16] F.C. Frank, *On spontaneous asymmetric synthesis*, *Biochim. Biophys. Acta* 11 (1953) 459–463.
- [17] D.K. Kondepudi, G.W. Nelson, *Weak neutral currents and the origin of biomolecular chirality*, *Nature* 314 (1985) 438–441.
- [18] D.K. Kondepudi, R.J. Kaufman, N. Singh, *Chiral symmetry breaking in sodium chlorate crystallization*, *Science* 250 (1990) 975–976.
- [19] K. Soai, T. Shibata, in: G. Pályi, C. Zucchi, L. Caglioti (Eds.), *Advances in Biochirality*, Elsevier, Amsterdam, 1999, p. 125.
- [20] K. Soai, T. Shibata, I. Sato, *Enantioselective automultiplication of chiral molecules by asymmetric autocatalysis*, *Acc. Chem. Res.* 33 (2000) 382–390.
- [21] J. Rivera Islas, V. Pimienta, J.C. Micheau, T. Buhse, *Kinetic analysis of artificial peptide self-replication. Part I: The homochiral case*, *Biophys. Chem.*, this issue.
- [22] D.H. Lee, J.R. Granja, J.A. Martinez, K. Severin, M.R. Ghadiri, *A self-replicating peptide*, *Nature* 382 (1996) 525–528.

- [23] K. Severin, D.H. Lee, J.A. Martinez, M.R. Ghadiri, Peptide self-replication via template-directed ligation, *Chem Eur. J.* 3 (1997) 1017–1024.
- [24] A. Saghatelian, Y. Yokobayashi, K. Soltani, M.R. Ghadiri, A chiroselective peptide replicator, *Nature* 409 (2001) 797–801.
- [25] Sa (Simulation + adjustment) is a non-commercial program based on C⁺⁺ that was developed at the Laboratoire de IMRCP, Université Paul Sabatier, Toulouse, France.
- [26] R. Issac, Y.-W. Ham, J. Chmielewski, The design of self-replicating helical peptides, *Curr. Opin. Struct. Biol.* 11 (2001) 458–463.
- [27] C. Micklatcher, J. Chmielewski, Helical peptide and protein design, *Curr. Opin. Chem. Biol.* 3 (1999) 724–729.
- [28] J. Jacques, A. Collet, S.H. Wilen, *Enantiomers, racemates and resolution*, Wiley, New York, 1981.
- [29] I. Bernal, Conglomerate crystallization and chiral discrimination phenomena, *J. Chem Educ.* 69 (1992) 468–469.
- [30] T. Buhse, D.K. Kondepudi, B. Hoskins, Kinetics of chiral resolution in stirred crystallization of D/L-glutamic acid, *Chirality* 11 (1999) 343–348.